Electronic excited state transport and trapping in solution

Roger F. Loring, Hans C. Andersen, and M. D. Fayer

Department of Chemistry, Stanford University, Stanford, California 94305
(Received 3 September 1981; accepted 19 October 1981)

A theoretical study of transport and trapping of electronic excitations in a two-component disordered system is carried out. The results are applicable to energy transport in solutions containing randomly distributed donor and trap solute species or lattices with randomly distributed donor and trap impurities. The diagrammatic expansion of the Green function, developed by Gochanour, Andersen, and Fayer to study excited state energy transport in a one-component system is applied to the trapping problem. The following quantities are calculated from the Green function: the time-dependent probabilities that an excitation is in the donor or in the trap ensembles, the generalized diffusion coefficient, and the mean-squared displacement of an excitation. For Förster transfer, transport properties are shown to depend on the ratio of the Förster interaction lengths R_0^{DT} and R_0^{DD} as well as on the reduced concentrations of donors and traps $[C_D = 4/3\pi(R_0^{DD})^3\rho_D,\ C_T = 4/3\pi\ (R_0^{DT})^3\rho_T]$. The tranport of excitations is found to be nondiffusive. A comparison to other theoretical treatments is presented.

I. INTRODUCTION

The problem of radiationless transport of electronic excitations in solutions containing traps was addressed by Förster over 30 years ago.[1] Trapping of electronic excitations is responsible for phenomena such as sensitized luminescence in crystals and solutions[2] and sensitized photochemistry such as photosynthesis.[3] The study of transport and trapping dynamics has also become an important tool for investigating biological[4] and polymer systems.[5] Förster considered solutions containing two solute species: donor molecules and traps. An electronic excitation could be transferred from donor to trap via a resonant dipole–dipole interaction. (Subsequently the work was extended to higher multipole and exchange interactions.[2,6]) Förster treated the case in which the trap concentration is much greater than the donor concentration. Each donor is assumed to interact only with an ensemble of neighboring traps, so transport from one donor to another is neglected. Förster and later workers[7] showed that in this limit, the time dependent probability that a donor molecule has retained its electronic excitation can be calculated exactly.

Recently, Huber has treated excited state transport in crystals containing donor and acceptor ions as randomly distributed dilute impurities.[8,9] Using a coherent potential approximation, he calculates the Laplace transform of the donor fluorescence decay. Huber argues that his approximations are valid for all values of the ratio of donor concentration to trap concentration, provided that the strength of interaction between donors is at least as large as the strength of interaction between donor and trap.

A convenient formulation of the problem of excited state transport in a one component disordered system has been given by Haan and Zwanzig.[10] They described the transport using a set of coupled rate equations, and determined that transport was nondiffusive at short times. This treatment was extended by Gochanour, Andersen, and Fayer, hereafter referred to as GAF, who used a diagrammatic technique to obtain an approximation to the Green function which included many high order terms.[11] Within their approximation, the transport becomes diffusive in the long time limit, and it is very likely that diffusion at long times is also a property of the exact solution of the problem.

In this work, we apply the diagrammatic techniques developed by GAF to the problem of trapping in disordered systems. The system under consideration here consists of immobile donor and trap molecules or ions dissolved in a host medium which does not participate in the excitation transport. Excitations can be transferred from donor to donor and donor to trap, but the trapping step is taken to be irreversible. Our formalism is general, and can be applied to any form of the molecular interaction. Here we specialize to the case of dipole–dipole interactions. Our goal is the calculation of the system's Green function, from which all of the trapping and transport properties of the system can be calculated.

In Sec. II, we present the master equation and Green function. In Sec. III, we outline the topological reduction of the Green function. A hierarchy of self-consistent approximations to the Green function is discussed in Sec. IV. We treat the calculation of experimental observables in Sec. V. Section VI contains the comparison of our results to other work.

II. THE MASTER EQUATION AND GREEN FUNCTION

The system consists of N donor molecules and M trap molecules randomly distributed in a volume Ω, with number densities ρ_D and ρ_T, respectively. The donor molecules are labeled 1 through N, and the trap molecules $N+1$ through $N+M$. The probability that an excitation is on the jth molecule in configuration $R = (\mathbf{r}_1, \mathbf{r}_2, \ldots, \mathbf{r}_{N+M})$ at time t, $p_j'(R, t)$, satisfies the master equation[8-11]

$$\frac{dp_j'}{dt} = \sum_{k=1}^{N} w_{jk}(p_k' - p_j') - \sum_{k=N+1}^{N+M} v_{kj}p_j' - p_j'/\tau_D\ ,\quad j \le N\ ,$$

$$\frac{dp_j'}{dt} = \sum_{k=1}^{N} v_{jk}p_k' - p_j'/\tau_T\ ,\quad N+1 \le j \le N+M\ . \tag{1}$$

The distance dependent transfer rates between two donor molecules and a donor molecule and a trap molecule are given by $w_{jk}(r_{jk})$ and $v_{jl}(r_{jl})$. The transfer rates are

 0021-9606/82/042015-13$02.10

taken to be independent of orientation and only dependent on distance. w_{jj} is defined to be zero. The donor–donor transfer rate is assumed to be symmetric: $w_{jk}=w_{kj}$. τ_D and τ_T are the measured lifetimes of the excitation on the donor and the trap, respectively, in the absence of intermolecular transfer. Later in this work, the results will be specialized to the orientation averaged Förster rate, applicable to a dipole–dipole interaction[12]

$$w_{jk}=\frac{1}{\tau_D}\left(\frac{R_0^{DD}}{r_{jk}}\right)^6 ,$$
$$v_{jk}=\frac{1}{\tau_D}\left(\frac{R_0^{DT}}{r_{jk}}\right)^6 . \tag{2}$$

The effects of including orientational factors in the transfer rate are discussed by Gochanour and Fayer.[13] In this model, transfer of excitations from trap to donor or trap to trap is forbidden. This is in accord with many well defined experimental situations.[14] Equation (1) is a valid description of this system if only a small fraction of the molecules is excited at any time, since transport will be affected if donors and traps near an excited donor are already excited.[8,15]

Initially we specialize to the case where the excitation lifetimes of both species are the same ($\tau_D=\tau_T=\tau$). If we give both species the donor lifetime, we will be able to conveniently calculate the donor dynamics, which are independent of the trap lifetime, since there is no back transfer. In Sec. V we show how to derive the trap dynamics from the donor dynamics if the lifetimes are different, so no generality is lost.

The decay term can be eliminated from Eq. (1) with the transformation

$$p_j(R,t)=p_j'(R,t)\exp(t/\tau) . \tag{3}$$

The resulting equation can be recast in matrix form

$$\frac{d\mathbf{p}(R,t)}{dt}=\mathbf{Q}\cdot\mathbf{p}(R,t) , \tag{4}$$

where $\mathbf{p}(R,t)$ is a vector with components $[p_1(R,t), p_2(R,t),\ldots,p_{N+M}(R,t)]$ and $\mathbf{Q}$ is an $N+M$ by $N+M$ matrix given by

$$Q_{jk}=w_{jk}-\delta_{jk}\left[\sum_{l=1}^{N}w_{lk}+\sum_{l=N+1}^{N+M}v_{lk}\right] , \quad j,k\le N ,$$
$$Q_{jk}=v_{jk} , \quad N+1\le j\le N+M,\ k\le N,$$
$$Q_{jk}=0 , \quad k>N . \tag{5}$$

Equation (4) has the formal solution[10]

$$\mathbf{p}(R,t)=\exp(t\mathbf{Q})\cdot\mathbf{p}(R,0) . \tag{6}$$

The quantity of interest here is the time and distance dependent ensemble averaged density of excitations

$$P(\mathbf{r},t)=\left\langle\sum_{j=1}^{N+M}\delta(\mathbf{r}_j-\mathbf{r})p_j(R,t)\right\rangle , \tag{7}$$

where the ensemble average of a function $A(R)$ is given by

$$\langle A(R)\rangle=\frac{1}{\Omega^{N+M}}\int d\mathbf{r}_1\cdots\int d\mathbf{r}_{N+M}A(R) . \tag{8}$$

The Green function $G(\mathbf{r},\mathbf{r}',t)$ is defined by

$$P(\mathbf{r},t)=\int d\mathbf{r}'\,G(\mathbf{r},\mathbf{r}',t)P(\mathbf{r}',0) . \tag{9}$$

The Green function gives the conditional probability of finding an excitation at position $\mathbf{r}$ and time t, given that it originated at position $\mathbf{r}'$ at time $t=0$. It is convenient to write $G(\mathbf{r},\mathbf{r}',t)$ as the sum of three terms

$$G(\mathbf{r},\mathbf{r}',t)=G^s(\mathbf{r}-\mathbf{r}',t)+G^m(\mathbf{r}-\mathbf{r}',t)+G^T(\mathbf{r}-\mathbf{r}',t) , \tag{10}$$

where

$$G^s(\mathbf{r}-\mathbf{r}',t)=\delta(\mathbf{r}-\mathbf{r}')\langle[\exp(t\mathbf{Q})]_{11}\rangle , \tag{11}$$
$$G^m(\mathbf{r}-\mathbf{r}',t)=(N-1)\langle\delta(\mathbf{r}_{12}-\mathbf{r}+\mathbf{r}')[\exp(t\mathbf{Q})]_{21}\rangle , \tag{12}$$
$$G^T(\mathbf{r}-\mathbf{r}',t)=M\langle\delta(\mathbf{r}_{1,N+1}-\mathbf{r}+\mathbf{r}')[\exp(t\mathbf{Q})]_{N+1,1}\rangle . \tag{13}$$

We assume that no traps are excited at $t=0$. The integral of $G^s(\mathbf{r}-\mathbf{r}',t)$ over a small volume about $\mathbf{r}'$ gives the probability that the excitation is still on the initial site at time t. $G^m(\mathbf{r}-\mathbf{r}',t)$ and $G^T(\mathbf{r}-\mathbf{r}',t)$ are measures of the probability of finding the excitation on a donor site other than the initial site and on a trap site, respectively.

We now carry out a diagrammatic expansion of $G(\mathbf{r}-\mathbf{r}',t)$, following the approach of GAF. It is convenient to work with the Laplace–Fourier transform of the Green function. The transform of $F(\mathbf{r},t)$ is given by

$$\hat{F}(\mathbf{k},\epsilon)=\int_0^\infty dt\,e^{-\epsilon t}\int d\mathbf{r}\exp(i\mathbf{k}\cdot\mathbf{r})F(\mathbf{r},t) . \tag{14}$$

Transforming Eqs. (11), (12), and (13) yields

$$\hat{G}^s(\epsilon)=\langle[(\epsilon\mathbf{I}-\mathbf{Q})^{-1}]_{11}\rangle , \tag{15}$$
$$\hat{G}^m(\mathbf{k},\epsilon)=(N-1)\langle\exp(i\mathbf{k}\cdot\mathbf{r}_{12})[(\epsilon\mathbf{I}-\mathbf{Q})^{-1}]_{21}\rangle , \tag{16}$$
$$\hat{G}^T(\mathbf{k},\epsilon)=M\langle\exp(i\mathbf{k}\cdot\mathbf{r}_{1,N+1})[(\epsilon\mathbf{I}-\mathbf{Q})^{-1}]_{N+1,1}\rangle , \tag{17}$$

where $\mathbf{I}$ is the unit matrix. We obtain the diagrammatic expansion of these functions by expanding the matrix $(\epsilon\mathbf{I}-\mathbf{Q})^{-1}$ in powers of ϵ and $\mathbf{Q}$. Each of these functions can then be written as the ensemble average of an infinite series of products of w_{ji} and v_{ji} factors. Each such product can be represented with a diagram as follows. Donor and trap sites are represented by circles and squares, respectively. A factor w_{ji} or v_{ji} is represented by a solid arrow from site i to site j, which can be thought of as an increase in probability on site j resulting from transfer from site i. A factor $-w_{ji}$ or $-v_{ji}$ is represented by a solid arrow from site i to site j, followed by a dashed arrow returning to site i. These factors correspond to a decrease in excitation probability on site i due to transfer of probability to site j. This shorthand is depicted in Fig. 1. Diagrams representing a product of w_{ji} and v_{ji} factors are constructed by connecting the arrows for consecutive factors head to tail. The point where two arrows connect will be called a vertex, if the arrow leaving the point is a solid arrow. The beginning and end points are also defined as vertices. The solid dots in Fig. 1 are vertices. A diagram representing a product of n Q_{ji} factors will have $n+1$ vertices. Since the product will be premultiplied by $n+1$ factors of ϵ^{-1}, each vertex is assigned a value ϵ^{-1}.

The diagrammatic expansion of $\hat{G}^s(\epsilon)$ can be written

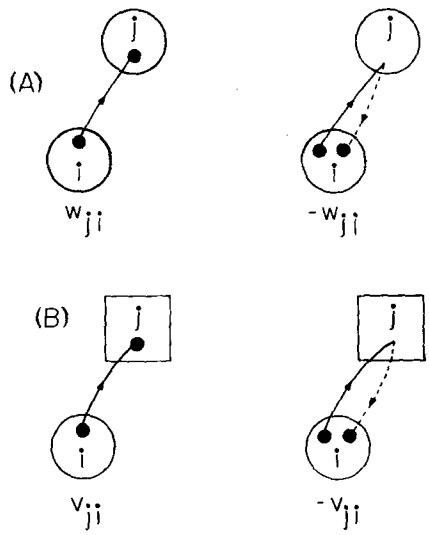

FIG. 1. Diagrammatic representations of the transfer rates w_{ji} and $-w_{ji}$ (A) and v_{ji} and $-v_{ji}$ (B).

$\hat{G}^s(\epsilon) = \epsilon^{-1}$ + the sum of all distinct diagrams which have a path of solid and dashed arrows beginning and ending on circle 1. (18)

Two diagrams are distinct if, when labeled with the same set of labels, there is no way of rearranging the labels to make the diagrams identical. The sites on which the path of arrows begins and ends are called root sites and the rest of the sites in a diagram are referred to as field sites. An nth order diagram is one with n solid arrows. The value of an nth order $\hat{G}^s(\epsilon)$ diagram with l donor field sites and m trap field sites is

$$\frac{\rho_D^l \rho_T^m}{\epsilon^{n+1}} \int d\mathbf{r}_{12} \cdots \int d\mathbf{r}_{1,N+M} \Pi(w_{ij}) \Pi(v_{ij}) \Pi(-1) , \tag{19}$$

where we have taken the thermodynamic limit ($N, M, \Omega \to \infty$, ρ_D, ρ_T constant). $\Pi(w_{ij})\Pi(v_{ij})\Pi(-1)$ indicates the appropriate product of transfer rates in Eqs. (19), (21), and (23). $\hat{G}^m(\mathbf{k}, \epsilon)$ is given by

$\hat{G}^m(\mathbf{k}, \epsilon)$ = the sum of all distinct diagrams with two donor root sites labeled 1 and 2 and zero or more field sites that have a path of solid and dashed arrows starting on site 1 and ending on site 2. (20)

The value of an nth order diagram with l donor field circles and m trap field circles is

$$\frac{\rho_D^{l+1} \rho_T^m}{\epsilon^{n+1}} \int d\mathbf{r}_{12} \cdots \int d\mathbf{r}_{1,l+1} \int d\mathbf{r}_{1,N+1} \cdots \int d\mathbf{r}_{1,N+m} \Pi(w_{ij}) \Pi(v_{ij}) \times \Pi(-1) \exp(i\mathbf{k} \cdot \mathbf{r}_{12}) . \tag{21}$$

$\hat{G}^T(\mathbf{k}, \epsilon)$ can be expressed as the following series

$\hat{G}^T(\mathbf{k}, \epsilon)$ = the sum of all distinct diagrams with a donor root site labeled 1 and a trap root site labeled $N+1$ and zero or more field sites that have a path of solid and dashed arrows starting on site 1 and ending on site $N+1$. (22)

In the thermodynamic limit, the value of an nth order diagram with l donor field sites and m trap field sites is given by

$$\frac{\rho_D^l \rho_T^{m+1}}{\epsilon^{n+1}} \int d\mathbf{r}_{12} \cdots \int d\mathbf{r}_{1,l+1} \int d\mathbf{r}_{1,N+1} \cdots \int d\mathbf{r}_{1,N+m} \times \Pi(w_{ij}) \Pi(v_{ij}) \Pi(-1) \exp(i\mathbf{k} \cdot \mathbf{r}_{1,N+1}) . \tag{23}$$

III. TOPOLOGICAL REDUCTION OF THE GREEN FUNCTION

In their treatment of excited state transport in a one component system, GAF are able to simplify their diagrammatic series for $\hat{G}^m(\mathbf{k}, \epsilon)$ by identifying two topological features of the diagrams: loops and nodes. A loop is a sequence of arrows beginning and ending on the same site. The sites visited on this path are not visited in any other part of the diagram. GAF show that the infinite set of diagrams that represent $\hat{G}^m(\mathbf{k}, \epsilon)$ can be generated from the set of all $\hat{G}^m(\mathbf{k}, \epsilon)$ diagrams without loops by assigning each vertex in the latter diagrams a value $\hat{G}^s(\epsilon)$. This simplification still holds for the system under consideration here, although the reduced set of diagrams without loops for the trapping problem consists of all of the diagrams discussed by GAF for the one component system plus a set of diagrams containing trap sites. Thus, Eq. (20) can be rewritten

$\hat{G}^m(\mathbf{k}, \epsilon)$ = the sum of all distinct diagrams with two donor root circles labeled 1 and 2, zero or more field circles, no loops, and that have a path of solid and dashed arrows starting on site 1 and ending on site 2. Each vertex is now assigned a value of $\hat{G}^s(\epsilon)$ rather than ϵ^{-1}. (24)

A node is a vertex in a donor field site which divides the sites in the diagram into three distinct classes: the set of sites visited before the node, the site containing the node, and the set of sites visited after the node. GAF show that a diagram with nodes can be formed by joining diagrams without nodes. If we define the series $\tilde{\Delta}[\mathbf{k}, \hat{G}^s(\epsilon)]$ by

$\tilde{\Delta}[\mathbf{k}, \hat{G}^s(\epsilon)]$ = the sum of all diagrams in Eq. (24) without nodes, (25)

then $\hat{G}^m(\mathbf{k}, \epsilon)$ is given by

$$\hat{G}^m(\mathbf{k}, \epsilon) = \tilde{\Delta}[\mathbf{k}, \hat{G}^s(\epsilon)] \Big/ \left\{ 1 - \frac{\tilde{\Delta}[\mathbf{k}, \hat{G}^s(\epsilon)]}{\hat{G}^s(\epsilon)} \right\} . \tag{26}$$

{Note that GAF work with a quantity $\tilde{\Sigma}[\mathbf{k}, \hat{G}^s(\epsilon)]$, which is our $\tilde{\Delta}[\mathbf{k}, \hat{G}^s(\epsilon)]$ divided by $\rho_D[\hat{G}^s(\epsilon)]^2$.} In this work, a quantity with a tilde superscript represents a sum of diagrams whose donor vertices are assigned a value $\hat{G}^s(\epsilon)$. Note that $\tilde{\Delta}[\mathbf{k}, \hat{G}^s(\epsilon)]$ depends on ϵ only through $\hat{G}^s(\epsilon)$ since each ϵ^{-1} vertex has been renormalized to a value $\hat{G}^s(\epsilon)$. The first terms of $\tilde{\Delta}[\mathbf{k}, \hat{G}^s(\epsilon)]$ are shown in Fig. 2.

The topological reduction of the $\hat{G}^T(\mathbf{k}, \epsilon)$ series defined in Eq. (22) is analogous to the simplification of $\hat{G}^m(\mathbf{k}, \epsilon)$ described above. The complete set of $\hat{G}^T(\mathbf{k}, \epsilon)$ diagrams can be generated from the subset of those diagrams with no loops by assigning to all of the donor site vertices a value of $\hat{G}^s(\epsilon)$. The final trap site vertex retains its original value of ϵ^{-1} since no loops are possible

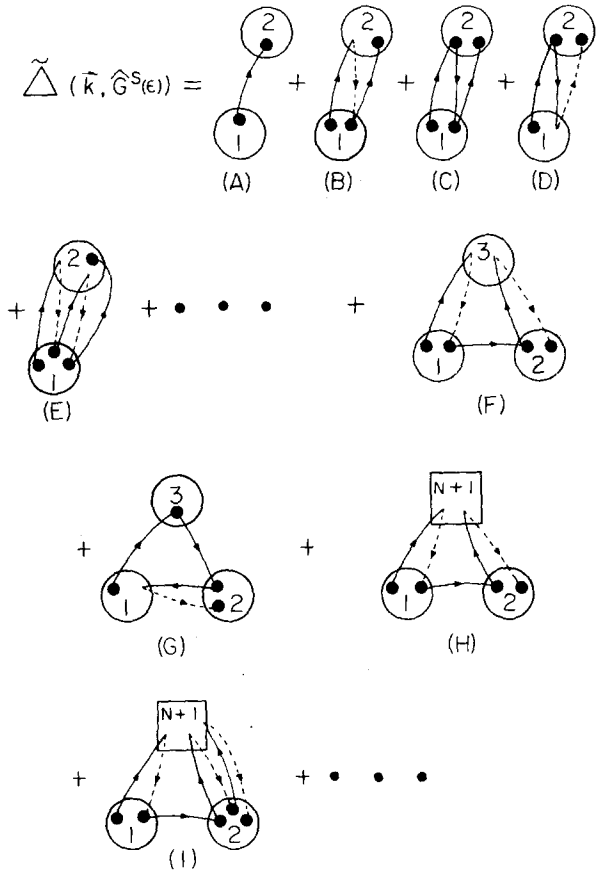

FIG. 2. Diagrammatic expansion of $\tilde{\Delta}[\mathbf{k}, \hat{G}^s(\epsilon)]$. Diagrams A–E are examples of two-body diagrams. Diagrams F–I are representative three-body diagrams.

which start on a trap, because transfer of excitation from a trap is forbidden. Equation (22) can then be rewritten as

$$\hat{G}^T(\mathbf{k}, \epsilon) = \text{the sum of all diagrams in Eq. (22) with no loops. Each donor vertex is assigned a value } \hat{G}^s(\epsilon) \text{ and the final trap vertex carries a value } \epsilon^{-1}. \quad (27)$$

The diagrams in Eq. (27) can be constructed from the subset of those diagrams containing no nodes with a procedure analogous to that used by GAF in their simplification of $\hat{G}^m(\mathbf{k}, \epsilon)$. We define $\tilde{\Gamma}[\mathbf{k}, \epsilon, \hat{G}^s(\epsilon)]$ as

$$\tilde{\Gamma}[\mathbf{k}, \epsilon, \hat{G}^s(\epsilon)] = \text{the sum of all diagrams in Eq. (27) with no nodes.} \quad (28)$$

The first terms of $\tilde{\Gamma}[\mathbf{k}, \epsilon, \hat{G}^s(\epsilon)]$ are shown in Fig. 3. A diagram in Eq. (27) with nodes can be broken into a series of uncorrelated transfers from node to node. The excitation visits a set of field sites, reaches a node, visits a new set of field sites, reaches a node, and so forth until it reaches the root trap site. Since transfer away from a trap is not allowed, all nodes must be donor vertices. Thus, a diagram in Eq. (27) with nodes can be represented by a product of several factors of $\tilde{\Delta}[\mathbf{k}, \hat{G}^s(\epsilon)]$, which represents paths from node to node, and a single factor of $\tilde{\Gamma}[\mathbf{k}, \epsilon, \hat{G}^s(\epsilon)]$, which represents the final path which the excitation follows from the last node to the trap. The complete set of diagrams in Eq. (27) is given by

$$\hat{G}^T(\mathbf{k}, \epsilon) = \tilde{\Gamma}[\mathbf{k}, \epsilon, \hat{G}^s(\epsilon)] / [1 - \tilde{\Delta}[\mathbf{k}, \hat{G}^s(\epsilon)] / \hat{G}^s(\epsilon)] . \quad (29)$$

We may now write the Laplace–Fourier transform of the total Green function in terms of $\hat{G}^s(\epsilon)$, $\tilde{\Delta}[\mathbf{k}, \hat{G}^s(\epsilon)]$, and $\tilde{\Gamma}[\mathbf{k}, \epsilon, \hat{G}^s(\epsilon)]$

$$\hat{G}(\mathbf{k}, \epsilon) = \hat{G}^s(\epsilon) + \hat{G}^m(\mathbf{k}, \epsilon) + \hat{G}^T(\mathbf{k}, \epsilon)$$
$$= \{\hat{G}^s(\epsilon) + \tilde{\Gamma}[\mathbf{k}, \epsilon, \hat{G}^s(\epsilon)]\} \Big/ \left\{1 - \frac{\tilde{\Delta}[\mathbf{k}, \hat{G}^s(\epsilon)]}{\hat{G}^s(\epsilon)}\right\} . \quad (30)$$

Let us consider the $k = 0$ limit of the Laplace–Fourier transform of the total Green function $\hat{G}(\mathbf{k}, \epsilon)$:

$$\lim_{k \to 0} \hat{G}(\mathbf{k}, \epsilon) = \lim_{k \to 0} \int_0^\infty e^{-\epsilon t}\, dt \int d\mathbf{r} \exp(i\mathbf{k} \cdot \mathbf{r}) G(\mathbf{r}, t)$$
$$= \int_0^\infty e^{-\epsilon t}\, dt \int d\mathbf{r}\, G(\mathbf{r}, t) . \quad (31)$$

Since $G(\mathbf{r}, t)$ is the solution to the master equation for the case of one initial excitation and since lifetime decay has been removed from the problem, the integral of $G(\mathbf{r}, t)$ over the total volume must equal unity at all times. Therefore,

$$\lim_{k \to 0} \hat{G}(\mathbf{k}, \epsilon) = 1/\epsilon . \quad (32)$$

In the $k = 0$ limit, Eq. (30) becomes

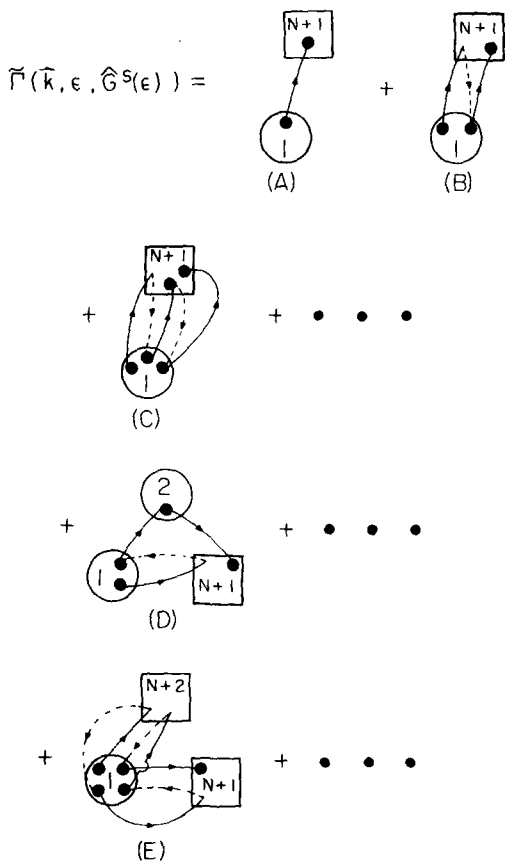

FIG. 3. Diagrammatic expansion of $\tilde{\Gamma}[\mathbf{k}, \epsilon, \hat{G}^s(\epsilon)]$. Diagrams A–C are representative two-body diagrams. Diagrams D and E are three-body diagrams with a donor field circle and a trap field circle, respectively.

$$\frac{1}{\epsilon}=\{\hat{G}^s(\epsilon)+\tilde{\Gamma}[0,\epsilon,\hat{G}^s(\epsilon)]\}\Big/\left\{1-\frac{\tilde{\Delta}[0,\hat{G}^s(\epsilon)]}{\hat{G}^s(\epsilon)}\right\}. \tag{33}$$

This equation is the basis for the self-consistent approximation applied in the next section.

IV. THE SELF-CONSISTENT APPROXIMATION: APPLICATION TO DIPOLE-DIPOLE TRANSFER

Equation (33) provides the basis for a self-consistent approximation to the function $\hat{G}^s(\epsilon)$, analogous to that derived by GAF. We take $\hat{G}^s(\epsilon)$ to be an unknown function. We partially sum the diagrammatic series for $\tilde{\Delta}[\mathbf{k}, \hat{G}^s(\epsilon)]$ and $\tilde{\Gamma}[\mathbf{k}, \epsilon, \hat{G}^s(\epsilon)]$ to get approximations to these functions in terms of the unknown $\hat{G}^s(\epsilon)$. If these approximations are substituted into Eq. (33), the resulting equation involves only known quantities and $\hat{G}^s(\epsilon)$, and hence can be solved for $\hat{G}^s(\epsilon)$. This self-consistent value for $\hat{G}^s(\epsilon)$ is then substituted into the partially summed series for $\tilde{\Delta}[\mathbf{k}, \hat{G}^s(\epsilon)]$ and $\tilde{\Gamma}[\mathbf{k}, \epsilon, \hat{G}^s(\epsilon)]$ to give approximations to these quantities. These approximations to $\tilde{\Delta}[\mathbf{k}, \hat{G}^s(\epsilon)]$ and $\tilde{\Gamma}[\mathbf{k}, \epsilon, \hat{G}^s(\epsilon)]$ can be substituted into Eqs. (26) and (29) to give approximations to $\hat{G}^m(\mathbf{k}, \epsilon)$ and $\hat{G}^T(\mathbf{k}, \epsilon)$. Thus, following GAF, instead of approximating $\hat{G}^s(\epsilon)$ directly from its diagrammatic series, we approximate $\tilde{\Delta}[\mathbf{k}, \hat{G}^s(\epsilon)]$ and $\tilde{\Gamma}[\mathbf{k}, \epsilon, \hat{G}^s(\epsilon)]$ and use the conservation of probability [Eq. (33)] to approximate $\hat{G}^s(\epsilon)$ self-consistently. We now consider the approximations to $\tilde{\Delta}[\mathbf{k}, \hat{G}^s(\epsilon)]$ and $\tilde{\Gamma}[\mathbf{k}, \epsilon, \hat{G}^s(\epsilon)]$.

The first terms of the diagrammatic expansion of $\tilde{\Delta}[\mathbf{k}, \hat{G}^s(\epsilon)]$ are shown in Fig. 2. The diagrams can be classified according to the number of sites in each diagram. We can write $\tilde{\Delta}[\mathbf{k}, \hat{G}^s(\epsilon)]$ as

$$\tilde{\Delta}[\mathbf{k}, \hat{G}^s(\epsilon)]=\sum_{n=2}^{\infty}\tilde{\Delta}_n[\mathbf{k}, \hat{G}^s(\epsilon)], \tag{34}$$

where $\tilde{\Delta}_n[\mathbf{k}, \hat{G}^s(\epsilon)]$ is the sum of all $\tilde{\Delta}[\mathbf{k}, \hat{G}^s(\epsilon)]$ diagrams with n sites. $\tilde{\Delta}_n[\mathbf{k}, \hat{G}^s(\epsilon)]$ will be referred to as the n-body term in $\tilde{\Delta}[\mathbf{k}, \hat{G}^s(\epsilon)]$. Similarly, we write

$$\tilde{\Gamma}[\mathbf{k}, \epsilon, \hat{G}^s(\epsilon)]=\sum_{n=2}^{\infty}\tilde{\Gamma}_n[\mathbf{k}, \epsilon, \hat{G}^s(\epsilon)], \tag{35}$$

where $\tilde{\Gamma}_n[\mathbf{k}, \epsilon, \hat{G}^s(\epsilon)]$ is the sum of all diagrams in Eq. (28) with n sites. $\tilde{\Gamma}_n[\mathbf{k}, \epsilon, \hat{G}^s(\epsilon)]$ will be referred to as the n-body term in $\tilde{\Gamma}[\mathbf{k}, \epsilon, \hat{G}^s(\epsilon)]$. It contains the exact summation of all unrenormalized diagrams with n sites plus contributions from higher order diagrams generated by the renormalization of the donor vertices.

The lowest order self-consistent approximation to the Green function is the two-body approximation, in which we retain only the two-body terms on the right sides of Eqs. (34) and (35)

$$\tilde{\Delta}[\mathbf{k}, \hat{G}^s(\epsilon)]=\tilde{\Delta}_2[\mathbf{k}, \hat{G}^s(\epsilon)], \tag{36}$$

$$\tilde{\Gamma}[\mathbf{k}, \epsilon, \hat{G}^s(\epsilon)]=\tilde{\Gamma}_2[\mathbf{k}, \epsilon, \hat{G}^s(\epsilon)]. \tag{37}$$

In this work we will also carry out the next order of approximation, the three-body approximation, in which we retain only the two- and three-body terms on the right sides of Eqs. (34) and (35)

$$\tilde{\Delta}[\mathbf{k}, \hat{G}^s(\epsilon)]=\tilde{\Delta}_2[\mathbf{k}, \hat{G}^s(\epsilon)]+\tilde{\Delta}_3[\mathbf{k}, \hat{G}^s(\epsilon)], \tag{38}$$

$$\tilde{\Gamma}[\mathbf{k}, \epsilon, \hat{G}^s(\epsilon)]=\tilde{\Gamma}_2[\mathbf{k}, \epsilon, \hat{G}^s(\epsilon)]+\tilde{\Gamma}_3[\mathbf{k}, \epsilon, \hat{G}^s(\epsilon)]. \tag{39}$$

It is important to realize the difference between the self-consistent n-body approximation to the Green function, and a truncated n-term density expansion. Because each vertex has the value $\hat{G}^s(\epsilon)$, each renormalized n-body diagram represents an infinite number of unrenormalized diagrams of higher order.

The determination of $\tilde{\Delta}_2[\mathbf{k}, \hat{G}^s(\epsilon)]$ is formally the same as the calculation of this quantity by GAF for a one component system, because both of the sites in all $\tilde{\Delta}_2[\mathbf{k}, \hat{G}^s(\epsilon)]$ diagrams must be donor sites. {Of course, the functional form of $\hat{G}^s(\epsilon)$ is different for the one component system than for the two component system because of the presence of trap sites in the latter case, but it is clear from the diagrammatic representations that the functional relationship between $\tilde{\Delta}_2[\mathbf{k}, \hat{G}^s(\epsilon)]$ and $\hat{G}^s(\epsilon)$ is the same for both problems.} GAF show that for the Förster transfer rate $\tilde{\Delta}_2[0, \hat{G}^s(\epsilon)]$ is given by

$$\tilde{\Delta}_2[0, \hat{G}^s(\epsilon)]=\frac{\pi}{2\sqrt{2}}C_D\tau^{-1/2}[\hat{G}^s(\epsilon)]^{3/2}. \tag{40}$$

The reduced concentration C_D is defined by

$$C_D=\tfrac{4}{3}\pi(R_0^{DD})^3\rho_D. \tag{41}$$

The calculation of $\tilde{\Gamma}_2[\mathbf{k}, \epsilon, \hat{G}^s(\epsilon)]$ follows along similar lines as the determination of $\tilde{\Delta}_2[\mathbf{k}, \hat{G}^s(\epsilon)]$ by GAF. We define

$$\tilde{\Gamma}_2[\mathbf{k}, \epsilon, \hat{G}^s(\epsilon)]=\sum_{n=1}^{\infty}\tilde{\Gamma}_2^n[\mathbf{k}, \epsilon, \hat{G}^s(\epsilon)], \tag{42}$$

where $\tilde{\Gamma}_2^n[\mathbf{k}, \epsilon, \hat{G}^s(\epsilon)]$ represents the sum of all diagrams in $\tilde{\Gamma}_2[\mathbf{k}, \epsilon, \hat{G}^s(\epsilon)]$ with n solid arrows. Since no back-transfer from traps is possible, $\tilde{\Gamma}_2^n[\mathbf{k}, \epsilon, \hat{G}^s(\epsilon)]$ consists of a single diagram with a sequence of a solid arrow to the trap followed by a dashed arrow returning to the donor repeated $n-1$ times, followed by a single solid arrow terminating in a trap vertex. The value of the $\tilde{\Gamma}_2^n[\mathbf{k}, \epsilon, \hat{G}^s(\epsilon)]$ diagram is easily determined from Eqs. (23) and (27) to be

$$\tilde{\Gamma}_2^n[\mathbf{k}, \epsilon, \hat{G}^s(\epsilon)]=\frac{1}{\epsilon}[\hat{G}^s(\epsilon)]^n\int d\mathbf{r}\,[v(\mathbf{r})]^n(-1)^{n-1}\exp(i\,\mathbf{k}\cdot\mathbf{r}). \tag{43}$$

The summation in Eq. (42) is carried out exactly to give

$$\tilde{\Gamma}_2[\mathbf{k}, \epsilon, \hat{G}^s(\epsilon)]=\frac{\rho_T\hat{G}^s(\epsilon)}{\epsilon}\int d\mathbf{r}\exp(i\,\mathbf{k}\cdot\mathbf{r})\frac{v(\mathbf{r})}{1+\hat{G}^s(\epsilon)v(\mathbf{r})}. \tag{44}$$

For the Förster rate and the $k=0$ limit, the integral can be evaluated analytically

$$\tilde{\Gamma}_2[0, \epsilon, \hat{G}^s(\epsilon)]=\frac{\pi}{2}\frac{C_T}{\epsilon}\left[\frac{\hat{G}^s(\epsilon)}{\tau}\right]^{1/2}. \tag{45}$$

The reduced concentration C_T is defined by

$$C_T=\tfrac{4}{3}\pi(R_0^{DT})^3\rho_T. \tag{46}$$

The two body approximation to $\hat{G}^s(\epsilon)$ is obtained by substituting Eqs. (40) and (45) into the self-consistent equation [Eq. (33)] to yield

$$\epsilon[\hat{G}^s(\epsilon)]+\left[\frac{\pi}{2}\tau^{-1/2}C_T+\frac{\pi}{2^{3/2}}\tau^{-1/2}C_D\right][\hat{G}^s(\epsilon)]^{1/2}-1=0, \tag{47}$$

TABLE I. Numerically evaluated integrals required in Eq. (49).

R_0^{DT}/R_0^{DD}	$\alpha(R_0^{DT}/R_0^{DD})$
0.1	7.8420×10^{-4}
0.2	6.2180×10^{-3}
0.5	7.9409×10^{-2}
0.6	1.1768×10^{-1}
0.8	1.8779×10^{-1}
1.0	2.3911×10^{-1}
2.0	3.3540×10^{-1}
3.0	3.5525×10^{-1}
5.0	3.6374×10^{-1}
10.0	3.6604×10^{-1}

TABLE II. Numerically evaluated integrals required in Eq. (50).

R_0^{DT}/R_0^{DD}	$\beta(R_0^{DT}/R_0^{DD})$
0.1	1.5683×10^{-3}
0.2	1.2415×10^{-2}
0.5	1.5703×10^{-1}
0.6	2.3534×10^{-1}
0.8	3.9408×10^{-1}
1.0	5.2990×10^{-1}
2.0	8.7595×10^{-1}
3.0	9.9053×10^{-1}
5.0	1.0666
10.0	1.1117

a quadratic equation in $[\hat{G}^s(\epsilon)]^{1/2}$. Only one of the two solutions to Eq. (47) will result in a $G^s(t)$, which is a decreasing function of time.

$$[\hat{G}^s(\epsilon)]^{1/2}=\frac{1}{2\epsilon}\left\{-\left[\frac{\pi}{2}\tau^{-1/2}C_T+\frac{\pi}{2^{3/2}}\tau^{-1/2}C_D\right]+\left[\left(\frac{\pi}{2}\tau^{-1/2}C_T+\frac{\pi}{2^{3/2}}\tau^{-1/2}C_D\right)^2+4\epsilon\right]^{1/2}\right\}. \quad (48)$$

The inverse Laplace transform of the square of this function gives the probability that an excitation is still on the initially excited molecule at some later time.

The calculation of $\tilde{\Gamma}_3[\mathbf{k},\epsilon,\hat{G}^s(\epsilon)]$ and $\tilde{\Delta}_3[\mathbf{k},\hat{G}^s(\epsilon)]$ is considerably more involved than the calculation of the two-body sums discussed above, and is outlined in the Appendix. The results of that calculation are presented here. $\tilde{\Delta}_3[0,\hat{G}^s(\epsilon)]$ is given by

$$\tilde{\Delta}_3[0,\hat{G}^s(\epsilon)]=-0.188\,70\,C_D^2\frac{[\hat{G}^s(\epsilon)]^2}{\tau}+\left[-0.383\,20+\alpha\left(\frac{R_0^{DT}}{R_0^{DD}}\right)\right]C_TC_D\frac{[\hat{G}^s(\epsilon)]^2}{\tau}. \quad (49)$$

$\tilde{\Delta}_3[0,\hat{G}^s(\epsilon)]$ has a contribution which depends on the ratio of the interaction strengths as well as the reduced concentrations. The function $\alpha(R_0^{DT}/R_0^{DD})$ is tabulated in Table I, and will be discussed further below. $\tilde{\Gamma}_3[0,\epsilon,\hat{G}^s(\epsilon)]$ also has a contribution which depends on the ratio R_0^{DD}/R_0^{DT}

$$\tilde{\Gamma}_3[0,\epsilon,\hat{G}^s(\epsilon)]=-0.337\,10\frac{C_T^2}{\epsilon\tau}\hat{G}^s(\epsilon)+\left[0.246\,04-\beta\left(\frac{R_0^{DT}}{R_0^{DD}}\right)\right]\frac{C_TC_D\hat{G}^s(\epsilon)}{\epsilon\tau}. \quad (50)$$

The function $\beta(R_0^{DT}/R_0^{DD})$ is tabulated in Table II.

Our next level of approximation is to set $\tilde{\Gamma}[\mathbf{k},\hat{G}^s(\epsilon)]$ equal to $\tilde{\Gamma}_2[\mathbf{k},\epsilon,\hat{G}^s(\epsilon)]+\tilde{\Gamma}_3[\mathbf{k},\epsilon,\hat{G}^s(\epsilon)]$, and $\tilde{\Delta}[\mathbf{k},\hat{G}^s(\epsilon)]$ equal to $\tilde{\Delta}_2[\mathbf{k},\hat{G}^s(\epsilon)]+\tilde{\Delta}_3[\mathbf{k},\hat{G}^s(\epsilon)]$ in Eq. (33), which gives a self-consistent equation for $\hat{G}^s(\epsilon)$ in the three-body approximation.

$$\left\{\epsilon-0.337\,10\frac{C_T^2}{\tau}-0.188\,70\frac{C_D^2}{\tau}-\left[0.137\,16-\alpha\left(\frac{R_0^{DT}}{R_0^{DD}}\right)+\beta\left(\frac{R_0^{DT}}{R_0^{DD}}\right)\right]\frac{C_TC_D}{\tau}\right\}[\hat{G}^s(\epsilon)]+\left[\frac{\pi}{2\tau^{1/2}}C_T+\frac{\pi}{2^{3/2}\tau^{1/2}}C_D\right][\hat{G}^s(\epsilon)]^{1/2}-1=0. \quad (51)$$

Like Eq. (47), this is a quadratic equation in $[\hat{G}^s(\epsilon)]^{1/2}$. Again, only one solution will give a $G^s(t)$, which is a monotonically decreasing function of time.

$$[\hat{G}^s(\epsilon)]^{1/2}=\left[-\left[\frac{\pi}{2\tau^{1/2}}C_T+\frac{\pi}{2^{3/2}\tau^{1/2}}C_D\right]+\left(\left[\frac{\pi}{2\tau^{1/2}}C_T+\frac{\pi}{2^{3/2}\tau^{1/2}}C_D\right]^2+4\left\{\epsilon-\frac{0.337\,10}{\tau}C_T^2-0.188\,70\frac{C_D^2}{\tau}-\left[0.137\,16-\alpha\left(\frac{R_0^{DT}}{R_0^{DD}}\right)+\beta\left(\frac{R_0^{DT}}{R_0^{DD}}\right)\right]\frac{C_TC_D}{\tau}\right\}\right)^{1/2}\right]\Big/\left(2\left\{\epsilon-\frac{0.337\,10\,C_T^2}{\tau}-\frac{0.188\,70\,C_D^2}{\tau}-\left[0.137\,16-\alpha\left(\frac{R_0^{DT}}{R_0^{DD}}\right)+\beta\left(\frac{R_0^{DT}}{R_0^{DD}}\right)\right]\frac{C_TC_D}{\tau}\right\}\right). \quad (52)$$

V. CALCULATION OF EXPERIMENTAL OBSERVABLES: DONOR AND TRAP DYNAMICS, TRANSPORT PROPERTIES

Two quantities which can be measured directly in time resolved studies of energy transport are the probabilities that an excitation is either on a donor or a trap at a given time after the system has been excited.[14] We define $G^D(\mathbf{r},t)$ as the probability that an excitation is on some donor site at position $\mathbf{r}$ and time t. Since the excitation may be either on the initially excited donor site or on another donor site, $G^D(\mathbf{r},t)$ must be the sum of the quantities $G^s(t)$ and $G^m(\mathbf{r},t)$. In the $k=0$ limit, the Laplace–Fourier transform of $G^D(\mathbf{r},t)$ is

$$\hat{G}^D(0,\epsilon)=\hat{G}^s(\epsilon)+\hat{G}^m(0,\epsilon). \quad (53)$$

Substituting Eq. (26) into Eq. (53) gives

$$\hat{G}^D(0,\epsilon)=\frac{[\hat{G}^s(\epsilon)]^2}{\hat{G}^s(\epsilon)-\tilde{\Delta}[0,\hat{G}^s(\epsilon)]}. \quad (54)$$

The probability that an excitation is somewhere in the donor ensemble as a function of time can be calculated by squaring Eq. (52) to obtain $\hat{G}^s(\epsilon)$, substituting this

function into Eqs. (40), (49), and (38) to obtain the three-body approximation to $\tilde{\Delta}[0, \hat{G}^s(\epsilon)]$, substituting those functions into Eq. (54), and then inverting the Laplace transform. In Fig. 4, we show representative plots of $G^D(t)$ [the inverse transform of Eq. (54)] in the two- and three-body approximations for $R_0^{DD}=R_0^{DT}$. The transform in Eq. (54) was inverted numerically, using the Stehfest method.[16] The fact that the two- and three-body curves are not very different suggests that the three body approximation is accurate. $G^D(t)$ depends only on the reduced concentrations in the two-body approximation, whereas it depends on both the reduced concentrations and the ratio R_0^{DT}/R_0^{DD} in the three-body approximation. In Fig. 5, we show the effect on $G^D(t)$ of keeping the reduced concentrations fixed and varying the relative interaction strengths.

The dependence on relative interaction strengths manifested in Fig. 5 is in marked contrast to other electronic transport situations. In the problem of transport in a one component system treated by GAF, the transport properties are only dependent on C, the reduced concentration. A reduction in interaction strength can be offset by an increased number density that keeps C constant. The system is insensitive to whether there are weak interactions and high number density or stronger interactions and fewer particles, as long as C is the same. The same situation is found in the Förster limit of the trapping problem. When C_D is vanishingly small, the trapping is determined strictly by C_T. However, in the trapping problem treated in this work, trapping depends on C_D, C_T, *and* R_0^{DT}/R_0^{DD}. Examining Fig. 5 shows that for fixed reduced concentrations and a given R_0^{DD}, trapping occurs faster with more traps having a weaker trapping interaction, i.e., more traps with smaller "capture volumes" $=\frac{4}{3}\pi(R_0^{DT})^3$. However, for fixed R_0^{DT} trapping occurs faster with fewer donors having larger "transfer volumes" $=\frac{4}{3}\pi(R_0^{DD})^3$.

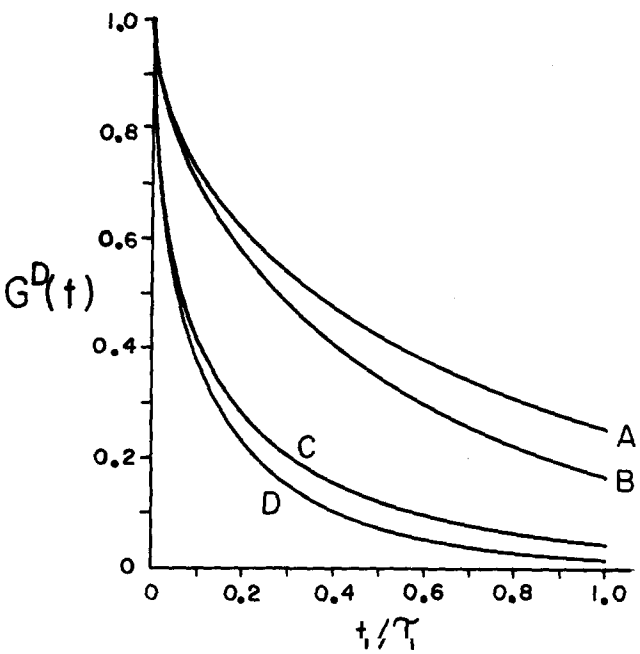

FIG. 4. The probability of an excitation remaining in the donor ensemble in the two-body and three-body approximations. $R_0^{DD}=R_0^{DT}$. A is the three-body result and B is the two-body result for $C_T=0.5$ and $C_D=1.5$. C is the three-body result and D is the two-body result for $C_T=1.5$ and $C_D=0.5$. Note that the decay is slower in the three-body approximation. Lifetime decay not included.

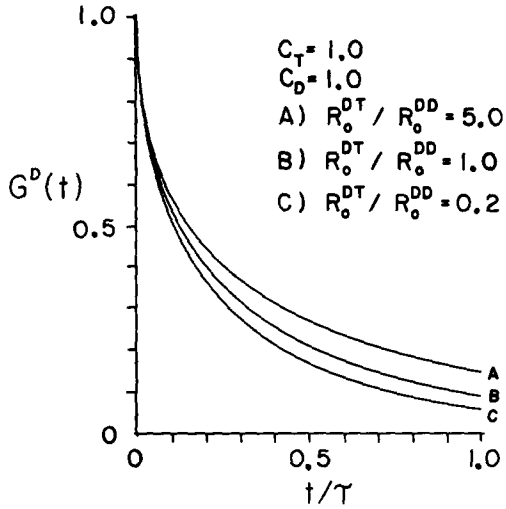

FIG. 5. The probability of an excitation remaining in the donor ensemble in the three-body approximation for fixed reduced concentrations and varying ratio of trap–donor and donor–donor interaction strengths. Lifetime decay is not included. This dependence on the ratio of interaction strengths for fixed reduced concentrations is not present in the two-body approximation.

In Eq. (3), we made the simplifying assumption that an excitation on a trap has the same lifetime as an excitation on a donor. This enabled us to eliminate lifetime decay from the problem. The inverse Laplace transform of Eq. (54) gives the probability that an excitation is in the donor ensemble for a system in which the excitation has an infinite lifetime on both species. If we wish to recover this probability for the situation in which the excitation has a finite lifetime τ_D on the donor, then the inverse transform of Eq. (54) must be multiplied by $\exp(-t/\tau_D)$. This procedure is valid regardless of whether the true trap lifetime equals the donor lifetime. The donor dynamics are independent of the trap lifetime, since back transfer from trap to donor does not occur.

The probability of finding an excitation somewhere in the trap ensemble at a given time after the donor has been excited can be calculated from Eq. (54), even if the excitation has different lifetimes on the donor and trap.

We define the following quantities:

$G^D(t)$ = the probability that the excitation is in the donor ensemble, if both species have infinite lifetimes. (55)

$G^T(t)$ = the probability that the excitation is in the trap ensemble if both species have infinite lifetimes. (56)

$N^D(t)$ = the probability that an excitation is on a donor if the donor lifetime is $1/k_D$. (57)

$N^T(t)$ = the probability that the excitation is on a trap if the donor lifetime is $1/k_D$ and the trap lifetime is $1/k_T$. (58)

$G^D(t)$ is the inverse Laplace transform of $\hat{G}^D(0, \epsilon)$, given in Eq. (54). $N^T(t)$ satisfies the equation

$$\dot{N}^T(t) = -k_T N^T(t) - e^{-k_D t}\dot{G}^D(t) , \tag{59}$$

where the first term is the probability loss due to the trap lifetime and the second term is the probability gain from the donors. If the Laplace transform of both sides of Eq. (59) is taken, using the initial conditions

$$N^T(0) = 0 , \qquad G^D(0) = 1 , \tag{60}$$

the result is

$$\hat{N}^T(\epsilon) = [1 - (\epsilon + k_D)\hat{G}^D(0, \epsilon + k_D)]/[\epsilon + k_T] . \tag{61}$$

$N^T(t)$ may be calculated by substituting Eq. (54) into Eq. (61), and performing the inverse transform.

The generalized diffusion coefficient and mean squared displacement of the excitation can be calculated from the Green function, as described by GAF. The relationship between the mean squared displacement of an excitation and the transient grating observable is discussed by GAF.

The Laplace–Fourier transform of the generalized diffusion coefficient $D(\mathbf{r}, t)$ is defined by the generalized diffusion equation[11,17]

$$\hat{G}(\mathbf{k}, \epsilon) = \frac{1}{\epsilon + k^2 D(\mathbf{k}, \epsilon)} . \tag{62}$$

For the present problem, it follows that $\hat{D}(\mathbf{k}, \epsilon)$ is

$$\hat{D}(\mathbf{k}, \epsilon) = \frac{1}{k^2}\left([\hat{G}^s(\epsilon)]^{-2}\{\tilde{\Delta}[0, \hat{G}^s(\epsilon)] - \tilde{\Delta}[\mathbf{k}, \hat{G}^s(\epsilon)]\} + \epsilon[\hat{G}^s(\epsilon)]^{-2}\{\tilde{\Gamma}[0, \epsilon, \hat{G}^s(\epsilon)]\tilde{\Delta}[\mathbf{k}, \hat{G}^s(\epsilon)] - \tilde{\Gamma}[\mathbf{k}, \epsilon, \hat{G}^s(\epsilon)]\tilde{\Delta}[0, \hat{G}^s(\epsilon)]\}\right.$$
$$\left. + \epsilon^2\{\tilde{\Gamma}[0, \epsilon, \hat{G}^s(\epsilon)] - \tilde{\Gamma}[\mathbf{k}, \epsilon, \hat{G}^s(\epsilon)]\}\right) \Big/ \left(1 + \frac{\tilde{\Delta}[0, \hat{G}^s(\epsilon)]}{[\hat{G}^s(\epsilon)]^2}\tilde{\Gamma}[\mathbf{k}, \epsilon, \hat{G}^s(\epsilon)] + \epsilon\{\tilde{\Gamma}[\mathbf{k}, \epsilon, \hat{G}^s(\epsilon)] - \tilde{\Gamma}[0, \epsilon, \hat{G}^s(\epsilon)]\}\right) . \tag{63}$$

The mean squared displacement is related to the Green function by

$$\langle r^2(t)\rangle = \int d\mathbf{r}\, r^2 G(\mathbf{r}, t) . \tag{64}$$

The Laplace transform of $\langle r^2(t)\rangle$ is given by

$$\langle r^2(\epsilon)\rangle = \frac{6}{\epsilon^2}\hat{D}(0, \epsilon) , \tag{65}$$

where

$$\hat{D}(0, \epsilon) = \lim_{k \to 0} \hat{D}(\mathbf{k}, \epsilon) . \tag{66}$$

To calculate the mean squared displacement in the two body approximation, we substitute Eq. (44) and the corresponding relation for $\tilde{\Delta}_2[\mathbf{k}, \hat{G}^s(\epsilon)]$ given by GAF into Eq. (63), and take the limit in Eq. (66). The mean squared displacement is then determined by substituting this expression into Eq. (65), and inverting the Laplace transform.[16] If transport becomes diffusive at long times, then the $\epsilon \to 0$ limit of $\hat{D}(0, \epsilon)$ must exist and be nonzero and the limiting value is the diffusion constant. GAF showed that a nonzero limit exists for a one component system in the two- and three-body approximations, and hence that transport is diffusive at long times within these approximations. Examination of Eq. (63) shows that

$$\lim_{\epsilon \to 0} \hat{D}(0, \epsilon) = 0 \tag{67}$$

for the trapping problem. Note that the $\epsilon \to 0$ limit of $\hat{G}^s(\epsilon)$ as defined in Eq. (48) or Eq. (52) exists, that $\tilde{\Delta}[\mathbf{k}, \hat{G}^s(\epsilon)]$ depends on ϵ only through $\hat{G}^s(\epsilon)$, and that $\tilde{\Gamma}[\mathbf{k}, \epsilon, \hat{G}^s(\epsilon)]$ is a function of $\hat{G}^s(\epsilon)$ multiplied by ϵ^{-1}. Equation (67) is to be expected, since at long times, the excitation will be trapped and will cease to move within the system. The mean squared displacement of the excitation will increase in a *nondiffusive* manner as a function of time until it reaches a value determined by donor and trap concentrations and interaction strengths. The mean squared displacement has a finite maximum value which is approached as $t \to \infty$. Transport is always nondiffusive in nature. Representative plots of the mean squared displacement and its derivative in the two-body approximation are given in Figs. 6(a) and 6(b). The three-body approximation to the mean squared displacement can be calculated by substituting Eqs. (38) and (39) into Eq. (63). The resulting three-body integrals can be evaluated with the approach outlined in the Appendix.

VI. COMPARISON TO OTHER WORK

The problem of excited state trapping in a disordered system where the trap concentration is much higher than the donor concentration and donor–donor transport can be neglected was solved exactly by Förster.[1] His result for the probability that the initially excited donor molecule is still excited at some later time is given by

$$\rho_D(t) = \exp(-C_D[\pi t/\tau]^{1/2}) , \tag{68}$$

where the lifetime decay of the donor has been suppressed. This quantity corresponds to our $G^D(t)$ in the limit that the donor concentration approaches zero. We can thus compare our two- and three-body approximations with the exact solution in this limit. Figure 7 shows a comparison of the two-body $G^D(t)$, the three-body $G^D(t)$, and Eq. (68). The three-body result is indistinguishable from the exact result for $C_T < 5$, and is very close for much higher concentrations.

Thus, it is clear that in the Förster limit, the diagrammatic self-consistent approximation to the Green function is extremely good. In the other limit, finite donor concentration but zero trap concentration, the current theory recovers analytically the results of GAF. The GAF results have been shown to be excellent ap-

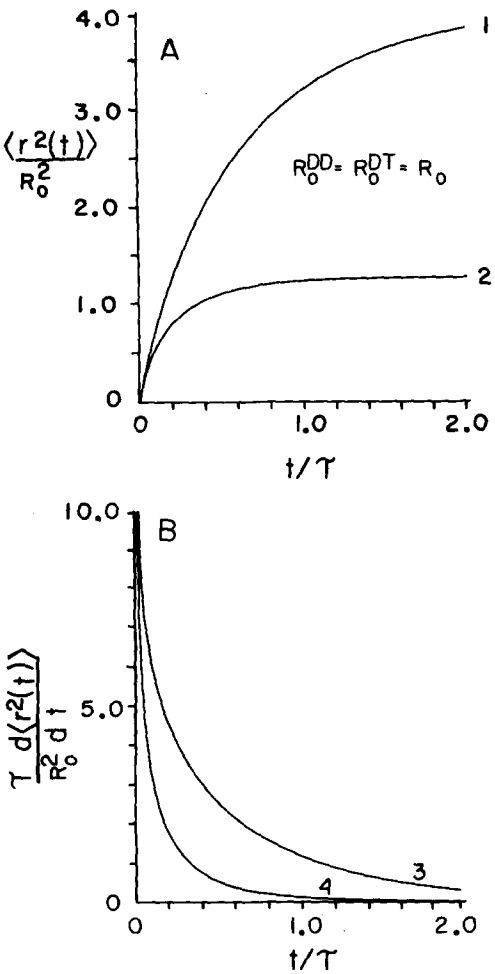

FIG. 6. (A) Mean squared displacements in the two-body approximation for $C_T = 0.5$, $C_D = 1.5$ (1), and $C_T = 1.5$, $C_D = 0.5$ (2). $R_0^{DD} = R_0^{DT}$. Lifetime decay not included. At long times, the mean squared displacement reaches a finite limit, since the excitation has been trapped. (B) Time derivatives of the mean squared displacements shown in A. (3) is the derivative of (1), and (4) is the derivative of (2). These curves emphasize the nondiffusive nature of the transport. The presence of traps causes these derivatives to go to zero at long times.

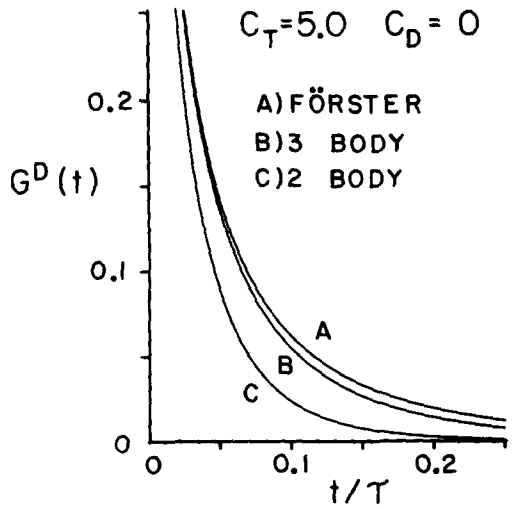

FIG. 7. Comparison of the two-body and three-body approximations in the limit of zero donor concentration to Förster's exact solution of this limiting case. The scales on both axes have been expanded so that the difference between the three-body approximation calculated here and the Förster result can be resolved. At $t/\tau = 0.1$, the three-body result differs from the Förster result by 0.007. The accuracy of the three-body approximation in this limit supports the validity of the general trapping theory presented here and suggests that the hierarchy of self-consistent approximations converges rapidly.

proximations, both by comparison to experiment[13] and by comparison to subsequent theoretical treatments using a continuous time random walk formalism.[18]

Huber has recently addressed the problem of the trapping of excitations in disordered systems.[8,9] Using an average t matrix formalism and a coherent potential approximation, he has derived an expression for a quantity corresponding to our $G^D(t)$, defined in Eq. (55). If the trap concentration is much lower than the donor concentration, this expression takes on a simple form

$$\hat{G}^D(0,\epsilon) = \left\{\epsilon + \frac{\pi}{2} C_T \left[\frac{1}{\tau \hat{G}^s(\epsilon)}\right]^{1/2}\right\}^{-1},$$
$$G^s(t) = \exp\left[-\left(\frac{\pi}{2\tau}\right)^{1/2} C_D t^{1/2}\right], \tag{69}$$

where we have rewritten the Huber results in the notation of this work. In Fig. 8 we compare the inverse transform[16] of Eq. (69) with our two- and three-body approximations to $G^D(t)$. Equation (69) lies between our two- and three-body results, though closer to the three-body curve.

Although Huber does not calculate the full Green function and has some restrictions on the conditions of applicability of the theory, the excellent agreement between the two theories when they are comparable strong-

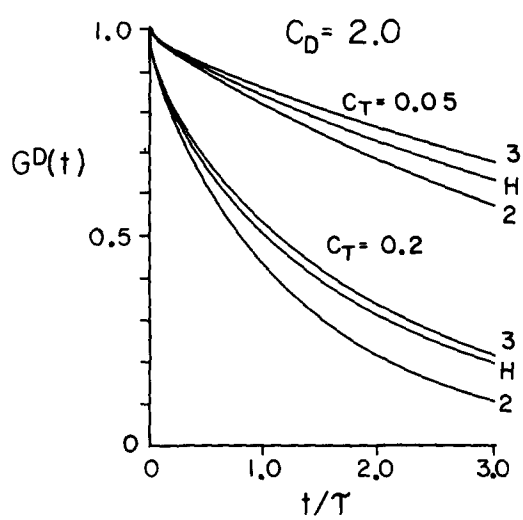

FIG. 8. Comparison of the two-body (2) and three-body (3) approximations to the results of Huber (H) in the limit of low trap concentration [see Eq. (69)]. Lifetime decay not included. $R_0^{DD} = R_0^{DT}$ in (2) and (3). The Huber results, formulated for the case $R_0^{DD} \geq R_0^{DT}$, depends on the interaction strengths only through the reduced concentrations, and does not display the dependence shown in Fig. 5. Under conditions for which comparison is possible, the two theories show good agreement.

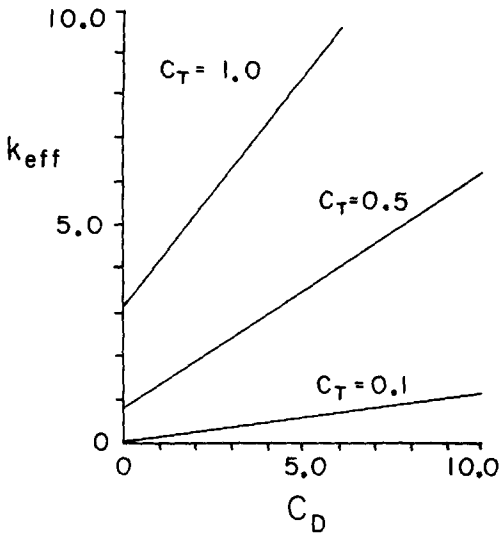

FIG. 9. The reciprocal of the time required for the nonexponential function $G^D(t)$ to fall to $1/e$ as a function of reduced donor concentration for fixed reduced trap concentration. The plots are very close to linear over the entire range of C_D.

ly supports their validity and the general validity and applicability of the present work. It is important to point out that Huber's theory does not reveal the dependence on the ratio R_0^{DT}/R_0^{DD} found here. In Fig. 8, the comparison was made with the ratio set equal to one.

In a recent experimental study, Lutz *et al.* examined the trapping of electronic excitations in Rhodamine 6G (R6G)-glycerol solutions by R6G dimers.[19] A simple model based on trapping of a random walker on a three dimensional lattice was put forward. Comparison with the present theory shows that the simple model predicts the correct functional dependence on concentration. Lutz *et al.* characterize the nonexponential decay of the donor population by an effective trapping rate constant defined by

$$k_{eff} = 1/t_e \,, \tag{70}$$

where t_e is the time for the donor population to fall to $1/e$ of its initial value. It is interesting to examine the concentration dependence of k_{eff} with the present theory. Figure 9 shows plots of k_{eff} as a function of donor concentration for several trap concentrations, obtained using Eq. (54). The dependence on C_D is very close to linear for each C_T. Actually, the plots have a very slight curvature which cannot be seen in the figure. The intercept is given by the Förster limit [Eq. (68)] obtained when C_D goes to zero.

The nearly linear dependence of k_{eff} on C_D can be understood very qualitatively by using random walk, site sampling arguments following Lutz *et al.*[19] If we consider each donor and trap molecule a site, then a walker will trap when it samples one trap site. The time for $G^s(t)$ to fall to $1/e$ is identified as the random walk step time. The decay of $G^s(t)$ scales approximately as C_D^2. As the donor concentration increases, the rate of sampling new sites increases approximately as C_D^2, but the number of sites which are not traps increases as C_D. Therefore, the overall rate of sampling a trap site increases nearly linearly with C_D as in Fig. 9. Figure 9 provides a simple method of visualizing and qualitatively applying the results of the theory. For a given trap concentration, the intercept can be calculated using Eq. (68), and then the necessary additional point to define the line is obtained from the inverse Laplace transform of Eq. (54). This type of plot can be extremely useful in designing and qualitatively interpreting experiments. It must be emphasized that the approximately linear dependence of k_{eff} on C_D does not give information on the functional form of the donor population decay, which is *nonexponential and not describable in terms of a trapping rate constant.*

ACKNOWLEDGMENTS

This work was supported by the National Science Foundation CHE 78-09317 and CHE 81-07165 (HCA) and DMR 79-20380 (MDF and RFL). In addition, RFL thanks the National Science Foundation for a Predoctoral Fellowship.

APPENDIX: CALCULATION OF THE THREE-BODY RESULTS

In this section, we outline the calculation of $\tilde{\Delta}_3[\mathbf{k}, \hat{G}^s(\epsilon)]$ and $\tilde{\Gamma}_3[\mathbf{k}, \epsilon, \hat{G}^s(\epsilon)]$ as defined in Eqs. (34) and (35). We need to sum the subsets of diagrams in $\hat{G}^m(\mathbf{k}, \epsilon)$ [Eq. (20)] and $\hat{G}^T(\mathbf{k}, \epsilon)$ [Eq. (22)] that have three sites and no loops or nodes. The sum of all $\hat{G}^m(\mathbf{k}, \epsilon)$ diagrams with three donor sites and no loops or nodes has already been evaluated by GAF. The result is included in Eq. (49). In evaluating the other sums, we follow the approach of GAF. To calculate each sum, we separately evaluate the sum of all three site diagrams, the sum of all three site diagrams with a loop, and the sum of all three site diagrams with a node, and then subtract the latter two quantities from the first.

First consider the evaluation of $\tilde{\Delta}_3''[\mathbf{k}, \hat{G}^s(\epsilon)]$, the sum of those diagrams in $\hat{G}^m(\mathbf{k}, \epsilon)$ with one trap site and no loops or nodes. Such a diagram may not have a node. We define

$III_A(\mathbf{k}, \epsilon)$ = the sum of all diagrams in $\hat{G}^m(\mathbf{k}, \epsilon)$ with two donor sites and one trap site. (A1)

$III_L(\mathbf{k}, \epsilon)$ = the sum of the subset of diagrams in Eq. (A1) with a loop. (A2)

Then

$$\tilde{\Delta}_3''[\mathbf{k}, \hat{G}^s(\epsilon)] = \tilde{III}_A[\mathbf{k}, \hat{G}^s(\epsilon)] - \tilde{III}_L[\mathbf{k}, \hat{G}^s(\epsilon)] \,, \tag{A3}$$

where $\tilde{III}_{A,L}$ is obtained from $III_{A,L}$ by replacing all ϵ^{-1} factors with $\hat{G}^s(\epsilon)$. As in Sec. III, a quantity with a tilde indicates a sum of diagrams whose donor vertices have been assigned a value $\hat{G}^s(\epsilon)$.

We now evaluate Eq. (A1). The first step is to write $\hat{G}^m(\mathbf{k}, \epsilon)$ as a density expansion for a system with a finite volume Ω, N donors, and M traps.

$$\hat{G}^m(\mathbf{k}, \epsilon) = \frac{N-1}{\Omega}\Lambda_m^{(1)}(\mathbf{k}, \epsilon, \Omega) + \frac{(N-1)(M)}{\Omega^2}\Lambda_m^{(2)}(\mathbf{k}, \epsilon, \Omega) + \cdots . \tag{A4}$$

$\hat{G}^m(\mathbf{k}, \epsilon)$ can be evaluated exactly for a system of two donors and a trap in a finite volume. Equating Eqs.

(16) and (A4) for this system gives

$$\Lambda_m^{(2)}(\mathbf{k},\epsilon,\Omega) = \Omega^2\langle\exp(i\mathbf{k}\cdot\mathbf{r}_{12})[\epsilon\mathbf{I}-\mathbf{Q}]^{-1}_{21}\rangle - \Omega\Lambda_m^{(1)}(\mathbf{k},\epsilon,\Omega)\ . \tag{A5}$$

$\Lambda_m^{(1)}(\mathbf{k},\epsilon,\Omega)$ is calculated by GAF from the exact solution to the problem of two donors in a finite volume. For three particles, the matrix $\epsilon\mathbf{I}-\mathbf{Q}$ in Eq. (A5) can be easily inverted. Equation (A5) then becomes

$$\Lambda_m^{(2)}(\mathbf{k},\epsilon,\Omega) = \int_\Omega d\mathbf{r}_{12}\int_\Omega d\mathbf{r}_{13}\exp[i\mathbf{k}\cdot\mathbf{r}_{12}]\left[\frac{w_{12}}{(\epsilon+w_{12}+v_{31})(\epsilon+w_{12}+v_{32})-w_{12}^2} - \frac{w_{12}}{\epsilon(\epsilon+2w_{12})}\right], \tag{A6}$$

where the two donors are labeled 1 and 2, and the trap is labeled 3. $\tilde{I}\tilde{I}\tilde{I}_A[\mathbf{k},\hat{G}^s(\epsilon)]$ is now calculated by taking the limit as $\Omega\to\infty$ of Eq. (A6), multiplying by $\rho_D\rho_T$, and replacing ϵ^{-1} with $\hat{G}^s(\epsilon)$. The diagrams composing $III_A(\mathbf{k},\epsilon)$ contain no trap vertices, so all vertices are renormalized to $\hat{G}^s(\epsilon)$. The result is

$$\tilde{I}\tilde{I}\tilde{I}_A[\mathbf{k},\hat{G}^s(\epsilon)] = \rho_D\rho_T\int d\mathbf{r}_{12}\int d\mathbf{r}_{13}\exp[i\mathbf{k}\cdot\mathbf{r}_{12}] \times\left(\frac{w_{12}}{\{[\hat{G}^s(\epsilon)]^{-1}+w_{12}+v_{31}\}\{[\hat{G}^s(\epsilon)]^{-1}+w_{12}+v_{32}\}-w_{12}^2} - \frac{w_{12}}{\{[\hat{G}^s(\epsilon)]^{-1}(2w_{12}+[\hat{G}^s(\epsilon)]^{-1})\}}\right). \tag{A7}$$

To solve the self-consistent equation [Eq. (33)] for $\hat{G}^s(\epsilon)$ in the three body limit, we need the $k=0$ limit of Eq. (A7). We define the integrand in Eq. (A7) with $k=0$ as $I(r_{12},r_{13},r_{23})$. $I(r_{12},r_{13},r_{23})$ is the sum of three terms

$$I(r_{12},r_{13},r_{23}) = F_1(r_{12},r_{13}) + F_2(r_{12},r_{23}) + R(r_{12},r_{13},r_{23})\ , \tag{A8}$$

where $F_1(r_{12},r_{13})$ and $F_2(r_{12},r_{23})$ result from setting v_{23} and v_{13}, respectively, equal to zero in $I(r_{12},r_{13},r_{23})$. The remainder, $R(r_{12},r_{13},r_{23})$ is defined by Eq. (A8). The integrals of $F_1(r_{12},r_{13})$ and $F_2(r_{12},r_{23})$ can be done analytically[20] and the integral of the remainder must be done numerically.

$$\rho_D\rho_T\int d\mathbf{r}_{12}\int d\mathbf{r}_{13}F_1(r_{12},r_{13}) = -\frac{\pi}{2^{3/2}}\frac{C_DC_T}{\tau}[\hat{G}^s(\epsilon)]^2E\left(\frac{\pi}{2},2^{-1/2}\right), \tag{A9}$$

where $E(\pi/2,2^{-1/2})$ is the complete elliptic integral of the second kind in the notation of Ref. 20. The integral of $F_2(r_{12},r_{23})$ is also given by Eq. (A9). The integral of $R(r_{12},r_{13},r_{23})$ was carried out by converting to bipolar coordinates,[21] and using an iterated Gaussian quadrature procedure. The result depends on the ratio of the interaction lengths as well as on the reduced concentrations. Combining this result with Eqs. (A7), (A8), and (A9) gives

$$\tilde{I}\tilde{I}\tilde{I}_A[0,\hat{G}^s(\epsilon)] = \frac{C_TC_D[\hat{G}^s(\epsilon)]^2}{\tau}[-3.0002+\alpha(R_0^{DT}/R_0^{DD})]\ , \tag{A10}$$

where the function $\alpha(R_0^{DT}/R_0^{DD})$ is tabulated in Table I.

Now consider the function $III_L(\mathbf{k},\epsilon)$, defined in Eq. (A2). Each diagram in this series has one loop connecting the initial donor site to the trap site. A diagram of this sort can be generated from a two site diagram in $\hat{G}^m(\mathbf{k},\epsilon)$, by assigning to one of the vertices on the initial donor the value of a two site diagram from the $\hat{G}^s(\epsilon)$ series [Eq. (18)], which contains a trap field site. The density expansion of $\hat{G}^s(\epsilon)$ in the thermodynamic limit is

$$\hat{G}^s(\epsilon) = \epsilon^{-1} + \rho_T\Lambda_s^{(1)}(\epsilon) + \rho_D\Lambda_s^{(2)}(\epsilon) + \cdots\ . \tag{A11}$$

$\Lambda_s^{(1)}(\epsilon)$ is the sum of all $\hat{G}^s(\epsilon)$ diagrams, with a single field site which is a trap. We can generate all of the diagrams in $III_L(\mathbf{k},\epsilon)$ from the set of two site diagrams in $\hat{G}^m(\mathbf{k},\epsilon)$ by sequentially replacing each ϵ^{-1} vertex on the initial donor site of each diagram with the value $\rho_T\Lambda_s^{(1)}(\epsilon)$. A two site $\hat{G}^m(\mathbf{k},\epsilon)$ diagram with two vertices labeled a and b on the first donor site will produce two diagrams in the $III_L(\mathbf{k},\epsilon)$ series. On one of these, vertex a will have the value $\rho_T\Lambda_s^{(1)}(\epsilon)$ and vertex b will have the value ϵ^{-1}, and on the other these assignments will be reversed. A two site diagram with n vertices on the initial donor will contribute n diagrams of equal value to the $III_L(\mathbf{k},\epsilon)$ series. The result is

$$III_L(\mathbf{k},\epsilon) = \frac{2\rho_D\rho_T}{\epsilon}\Lambda_s^{(1)}(\epsilon)\int d\mathbf{r}_{12}\frac{w_{12}(1+w_{12}/\epsilon)}{(1+2w_{12}/\epsilon)^2}\exp[i\mathbf{k}\cdot\mathbf{r}_{12}]\ . \tag{A12}$$

$\Lambda_s^{(1)}(\epsilon)$ can be calculated from the exact solution of one donor and one trap in a finite volume. Substituting this result into Eq. (A12) and replacing all ϵ^{-1} factors with $\hat{G}^s(\epsilon)$, we arrive at

$$\tilde{I}\tilde{I}\tilde{I}_L[\mathbf{k},\hat{G}^s(\epsilon)] = \frac{\pi\rho_DC_T}{[\hat{G}^s(\epsilon)]^{5/2}\tau^{1/2}} \times\int d\mathbf{r}_{12}\exp(i\mathbf{k}\cdot\mathbf{r}_{12})\frac{w_{12}[1+\hat{G}^s(\epsilon)w_{12}]}{[1+2\hat{G}^s(\epsilon)w_{12}]^2}\ . \tag{A13}$$

To determine $\tilde{I}\tilde{I}\tilde{I}_L[0,\hat{G}^s(\epsilon)]$, we set $k=0$ in Eq. (A13). The resulting integral over r_{12} can be done analytically[20] to yield

$$\tilde{I}\tilde{I}\tilde{I}_L[0,\hat{G}^s(\epsilon)] = -\frac{3\pi^2}{2^{7/2}}C_TC_D\frac{[\hat{G}^s(\epsilon)]^2}{\tau}\ . \tag{A14}$$

The function $\tilde{\Delta}_3''[0,\hat{G}^s(\epsilon)]$ can now be calculated from Eqs. (A3), (A10), and (A14):

$$\tilde{\Delta}_3''[0,\hat{G}^s(\epsilon)] = C_TC_D\frac{[\hat{G}^s(\epsilon)]^2}{\tau}\left[-0.383\,12+\alpha\left(\frac{R_0^{DT}}{R_0^{DD}}\right)\right]. \tag{A15}$$

We divide $\tilde{\Gamma}_3[\mathbf{k},\epsilon,\hat{G}^s(\epsilon)]$ into two sums: the sum of all diagrams with one trap site is labeled $\tilde{\Gamma}_3'[\mathbf{k},\epsilon,\hat{G}^s(\epsilon)]$, and the sum of those diagrams with two trap sites is labeled $\tilde{\Gamma}_3''[\mathbf{k},\epsilon,\hat{G}^s(\epsilon)]$. The calculation of $\tilde{\Gamma}_3'[\mathbf{k},\epsilon,\hat{G}^s(\epsilon)]$ is carried out with the same approach as the calculation of

$\tilde{\Delta}_3''[\mathbf{k}, \hat{G}^s(\epsilon)]$ above. The principal difference between the two procedures is that a three site diagram in $\tilde{\Delta}_3''[\mathbf{k}, \hat{G}^s(\epsilon)]$ with one trap site cannot have a node, whereas a three site diagram in $\tilde{\Gamma}_3'[\mathbf{k}, \epsilon, \hat{G}^s(\epsilon)]$ with one trap site can. In analogy to Eqs. (A1) and (A2), we define

$III_A'(\mathbf{k}, \epsilon)$ = the sum of all diagrams in $\hat{G}^T(\mathbf{k}, \epsilon)$ with two donor sites and one trap site, (A16)

$III_L'(\mathbf{k}, \epsilon)$ = the sum of all diagrams in Eq. (A16) with a loop, (A17)

$III_N'(\mathbf{k}, \epsilon)$ = the sum of all diagrams in Eq. (A16) with a node, (A18)

$$\tilde{\Gamma}_3'[\mathbf{k}, \epsilon, \hat{G}^s(\epsilon)] = \tilde{I}\tilde{I}\tilde{I}_A[\mathbf{k}, \epsilon, \hat{G}^s(\epsilon)] - \tilde{I}\tilde{I}\tilde{I}_L[\mathbf{k}, \epsilon, \hat{G}^s(\epsilon)] - \tilde{I}\tilde{I}\tilde{I}_N[\mathbf{k}, \epsilon, \hat{G}^s(\epsilon)] . \quad (A19)$$

The right-hand side of Eq. (A16) is evaluated with the same strategy used on Eq. (A1): by expanding $\hat{G}^T(\mathbf{k}, \epsilon)$ in a density expansion, and solving the two and three particle finite volume problems exactly. The result is

$$\tilde{I}\tilde{I}\tilde{I}_A'[\mathbf{k}, \epsilon, \hat{G}^s(\epsilon)] = \frac{\rho_T \rho_D}{\epsilon} \int d\mathbf{r}_{12} \exp(i\mathbf{k}\cdot\mathbf{r}_{12}) \int d\mathbf{r}_{13} \times \left(\frac{v_{32}w_{12} + v_{31}\{[\hat{G}^s(\epsilon)]^{-1} + w_{12} + v_{32}\}}{\{[\hat{G}^s(\epsilon)]^{-1} + w_{12} + v_{31}\}} - \frac{v_{31}}{\{[\hat{G}^s(\epsilon)]^{-1} + v_{31}\}} \right) . \quad (A20)$$

$\tilde{I}\tilde{I}\tilde{I}_A'[0, \epsilon, \hat{G}^s(\epsilon)]$ is evaluated using the approach described in Eq. (A8). Again, the two integrals over functions of two variables can be done analytically[20] and the remainder must be integrated numerically, with the result

$$\tilde{I}\tilde{I}\tilde{I}_A'[0, \epsilon, \hat{G}^s(\epsilon)] = \frac{C_D C_T}{\epsilon_T} \hat{G}^s(\epsilon)[1.11839 + \beta(R_0^{DT}/R_0^{DD})] . \quad (A21)$$

The function $\beta(R_0^{DT}/R_0^{DD})$ is tabulated in Table II.

$III_L'(\mathbf{k}, \epsilon)$ is evaluated using the same techniques that were applied to $III_L(\mathbf{k}, \epsilon)$. The set of diagrams composing $III_L'(\mathbf{k}, \epsilon)$ can be generated from the set of all two site diagrams in $\hat{G}^T(\mathbf{k}, \epsilon)$ with ϵ^{-1} vertices, and the function $\Lambda_s^{(2)}(\epsilon)$ defined in Eq. (A11). The same procedure that led to Eq. (A12) then gives

$$\tilde{I}\tilde{I}\tilde{I}_L'[\mathbf{k}, \epsilon, \hat{G}^s(\epsilon)] = \frac{\rho_T \rho_D \Lambda_s^{(2)}(\epsilon)}{\epsilon} \int d\mathbf{r}_{13} \exp(i\mathbf{k}\cdot\mathbf{r}_{13}) \frac{v_{31}}{\left(1 + \frac{v_{31}}{\epsilon}\right)^2} . \quad (A22)$$

$\Lambda_s^{(2)}(\epsilon)$ is calculated by GAF from the exact solution to the two particle finite volume problem. Substituting this result into Eq. (A22) and replacing all but one ϵ^{-1} factor with $\hat{G}^s(\epsilon)$ gives an expression for $\tilde{I}\tilde{I}\tilde{I}_L'[\mathbf{k}, \epsilon, \hat{G}^s(\epsilon)]$. $\tilde{I}\tilde{I}\tilde{I}_L'[0, \epsilon, \hat{G}^s(\epsilon)]$ may be evaluated analytically[20]

$$\tilde{I}\tilde{I}\tilde{I}_L'[0, \epsilon, \hat{G}^s(\epsilon)] = -\frac{C_D C_T}{\epsilon_T} \left(\frac{\pi^2}{2^{7/2}} \right) \hat{G}^s(\epsilon) . \quad (A23)$$

Following the approach of GAF, we find that the sum of all $\hat{G}^T(\mathbf{k}, \epsilon)$ diagrams with one node and no loops is

$$\hat{G}_1^T(\mathbf{k}, \epsilon) = \epsilon \Gamma(\mathbf{k}, \epsilon) \Delta(\mathbf{k}, \epsilon) , \quad (A24)$$

where $\Gamma(\mathbf{k}, \epsilon)$ and $\Delta(\mathbf{k}, \epsilon)$ are defined as in Eqs. (28) and (25), except that all vertices have the value ϵ^{-1}. The subset of diagrams in Eq. (A24) with three sites can be generated by replacing $\Gamma(\mathbf{k}, \epsilon)$ with $\Gamma_2(\mathbf{k}, \epsilon)$ and $\Delta(\mathbf{k}, \epsilon)$ with $\Delta_2(\mathbf{k}, \epsilon)$. In the $k = 0$ limit, we can use the results given in Eqs. (40) and (45). Replacing all but one ϵ^{-1} factor with $\hat{G}^s(\epsilon)$ yields

$$\tilde{I}\tilde{I}\tilde{I}_N'[0, \epsilon, \hat{G}^s(\epsilon)] = \frac{\pi^2}{2^{5/2}\epsilon_T} \hat{G}^s(\epsilon) C_D C_T . \quad (A25)$$

Substituting Eqs. (A21), (A23), and (A25) into Eq. (A19) gives

$$\tilde{\Gamma}_3'[0, \epsilon, \hat{G}^s(\epsilon)] = \frac{\hat{G}^s(\epsilon) C_D C_T}{\epsilon_T} [0.24604 + \beta(R_0^{DT}/R_0^{DD})] . \quad (A26)$$

The final quantity needed in the three body self-consistent approximation of $\hat{G}^s(\epsilon)$ is $\tilde{\Gamma}_3''[0, \epsilon, \hat{G}^s(\epsilon)]$, the sum of those $\hat{G}^T(\mathbf{k}, \epsilon)$ diagrams with two trap sites and one donor site, which have neither loops nor nodes. The calculation of this term is straightforward, and follows the procedure outlined above. Because transfer from a trap is forbidden, these diagrams may have loops but not nodes. Because of the simple nature of these diagrams, the integrals arising in this calculation can be done analytically.[20] The final result is

$$\tilde{\Gamma}_3''[0, \epsilon, \hat{G}^s(\epsilon)] = \frac{\pi^2 - 4\pi}{8} \frac{C_T^2}{\epsilon_T} [\hat{G}^s(\epsilon)] . \quad (A27)$$

Combining Eqs. (A26) and (A27) gives

$$\tilde{\Gamma}_3[0, \epsilon, \hat{G}^s(\epsilon)] = -\frac{0.33710 C_T^2}{\epsilon_T} \hat{G}^s(\epsilon) + \left[0.24604 + \beta\left(\frac{R_0^{DT}}{R_0^{DD}} \right) \right] \frac{C_T C_D}{\epsilon_T} \hat{G}^s(\epsilon) . \quad (A28)$$

[1] Th. Förster, Z. Naturforsch. Teil A **4**, 321 (1949).
[2] D. L. Dexter, J. Chem. Phys. **21**, 836 (1953).
[3] (a) R. M. Pearlstein, Proc. Natl. Acad. Sci. U.S.A. **52**, 824 (1964); (b) T. Markvart, J. Theor. Biol. **72**, 91 (1978); (c) G. Porter, Proc. R. Soc. London Ser. A **362**, 281 (1978).
[4] (a) E. Haas, M. Wilchek, E. Katachalski-Katzir, and I. Z. Steinberg, Proc. Natl. Acad. Sci. U.S.A. **72**, 1807 (1975); (b) R. E. Dale and J. Eisinger, *ibid.* **73**, 271 (1976).
[5] W. Klöpffer, Ann. NY Acad. Sci. **366**, 373 (1981).
[6] M. Inokuti and F. Hirayama, J. Chem. Phys. **43**, 1978 (1965).
[7] (a) M. D. Galanin, Sov. Phys. JETP **1**, 317 (1955); (b) M. Leibowitz, J. Phys. Chem. **69**, 1061 (1965); (c) U. Gösele, M. Hauser, and U. K. A. Klein, Z. Phys. Chem. **99**, 81 (1976).
[8] D. L. Huber, Phys. Rev. B **20**, 2307 (1979).
[9] D. L. Huber, Phys. Rev. B **20**, 5333 (1979).
[10] S. W. Haan and R. Zwanzig, J. Chem. Phys. **68**, 1879 (1978).
[11] C. R. Gochanour, H. C. Andersen, and M. D. Fayer, J. Chem. Phys. **70**, 4254 (1979).
[12] Th. Förster, Ann. Phys. (Leipzig) **2**, 55 (1948).
[13] C. R. Gochanour and M. D. Fayer, J. Phys. Chem. **85**, 1989 (1981).
[14] (a) G. Porter and C. J. Tredwell, Chem. Phys. Lett. **56**, 278 (1978); (b) D. P. Millar, R. J. Robbins, and A. H. Zewail, J. Chem. Phys. **75**, 3649 (1981); (c) Raoul Kopelman, J. Phys. Chem. **80**, 2191 (1976).
[15] S. K. Lyo, T. Holstein, and R. Orbach, Phys. Rev. B **18**, 1637 (1978).

[16]H. Stehfest, Commun. ACM **13**, 47 (1970); **13**, 624 (1970).
[17]D. Förster, *Hydrodynamics, Fluctuations, Broken Symmetry, and Correlation Functions* (Benjamin, London, 1975).
[18](a) J. Klafter and R. Silbey, J. Chem. Phys. **72**, 843 (1980); (b) K. Godzik and J. Jortner, *ibid.* **72**, 4471 (1980).
[19]D. R. Lutz, Keith A. Nelson, C. R. Gochanour, and M. D. Fayer, Chem. Phys. **58**, 289 (1981).
[20]I. S. Gradshteyn and I. M. Ryzhik, *Table of Integrals, Series and Products* (Academic, New York, 1965).
[21]Terrell L. Hill, *Statistical Mechanics* (McGraw–Hill, New York, 1956), pp. 203–204; S. W. Haan, Ph.D. thesis, University of Maryland, College Park, Maryland, 1977.